Molecular Structure of Dimethyl Sulfoxide Intercalated Kaolinites

Ray L. Frost,*,† Janos Kristof,‡ Gina N. Paroz,† and J. Theo Kloprogge†

Centre for Instrumental and Developmental Chemistry, Queensland University of Technology, 2 George Street, GPO Box 2434, Brisbane Queensland 4001, Australia, Department of Analytical Chemistry, University of Veszprem, H8201 Veszprem, PO Box 158, Hungary

Received: April 28, 1998; In Final Form: July 23, 1998

Upon the intercalation of kaolinite with DMSO, new Raman bands at 3660, 3536, and 3501 cm^{-1} are observed for the low-defect kaolinite and at 3664, 3543, and 3509 cm^{-1} for the high-defect kaolinite. An additional band at 3598 cm^{-1} was observed for the high-defect kaolinite. The band at 3660 cm^{-1} was assigned to the inner-surface hydroxyls hydrogen bonded to the S═O group. The other three bands are attributed to the hydroxyl stretching frequencies of water in the intercalation complex. The hydroxyl deformation region is characterized by one intense band in both the FTIR and Raman spectra at 905 cm^{-1}. Significant changes in the Raman spectra of the intercalating molecule are observed. Splitting of the C−H symmetric and antisymmetric stretching vibrations occurs. Two Raman bands at 2917 and 2935 cm^{-1} and four bands at 2999, 3015, 3021, and 3029 cm^{-1} are observed. The in-plane methyl bending region shows two Raman bands at 1411 and 1430 cm^{-1}. The DRIFT spectra show complexity in these regions. The S═O stretching region shows bands at 1066, 1023, and 1010 cm^{-1} upon intercalation with DMSO for the low-defect kaolinite and 1058, 1028, and 1004 cm^{-1} for the high-defect kaolinite. The 1058 cm^{-1} band is assigned to the free monomeric S═O group and the 1023 and 1010 cm^{-1} bands to two different polymeric S═O groups. Bands attributed to the C−S stretching vibrations, the in-plane and out-of-plane S═O bending and the CSC symmetric bends all move to higher frequencies upon intercalation. It is proposed that intercalation with DMSO depends on the presence of water and that the additional bands at 3536 and 3501 cm^{-1} are due to the presence of water in the intercalate.

Introduction

The intercalation of dimethyl sulfoxide (DMSO) into clay minerals has been used to separate the chlorite fractions from the kaolin minerals.[1−4] The reason DMSO is so successful at separating the clay minerals is that the kaolins expand from 7.2 to 11.2 Å. This expansion of the kaolin minerals by DMSO followed by deintercalation results in an increase in the stacking disorder of the kaolin.[5] Intercalation of DMSO into kaolinite provides a method for the incorporation of other alkali and alkaline metal salts into the kaolin by replacement of the DMSO.[6,7] When the kaolinite is expanded with DMSO, a three-dimensional ordering incorporating the DMSO into the interlamellar space occurs.[8,9] It has been proposed that when this three-dimensional ordering occurs, the DMSO molecule is locked into the kaolinite surfaces first by hydrogen bonding of the S═O to the gibbsite-like hydroxyls and by a coordination of the sulfur to the oxygens of the siloxane surface.[8] Such three-dimensional ordering then alters the molecular motion of the methyl groups of the DMSO.[10−14] Each DMSO molecule is triply hydrogen bonded above the octahedral vacancy in the gibbsitic sheet of the kaolinite layer. One methyl group is keyed into the ditrigonal hole in the tetrahedral sheet with the other S−C bond parallel to the sheet. The DMSO molecules are accommodated by significant horizontal displacement of individual kaolinite layers to achieve almost perfect overlap of the octahedral vacancy by the adjacent ditrigonal hole.[9]

Stable, 3-dimensionally ordered complexes were formed from synthetically hydrated, highly ordered kaolinite [d(001) = 8.40 Å] with DMSO.[15−17] Removal of the intercalated organic compounds by drying or by water washing produced an 8.40 Å hydrate with its ordered layer stacking essentially unchanged. The question may be raised as to why these hydrated kaolinites were formed. Isolated water molecules appear to be keyed into the ditrigonal holes formed by the basal O of the silicate tetrahedra of the 8.4 Å hydrate. These water molecules, referred to as "hole water", and ions that had replaced approximately 20% of the inner-surface OH groups of the 8.4 Å phase sufficiently altered the interlayer bonding to allow an expansion of the inner-layer spaces by a variety of guest molecules. Further, a 10 Å hydrated kaolin was produced. Hydrated kaolinite, with d(001) = 10 Å, was synthesized by mild heating of a kaolinite−DMSO suspension, allowing time for the clay to be intercalated, and then dissolving a fluoride salt in the solution. After mild heating of the suspension, the salt and DMSO are removed by repeated water washings. The kaolinite retained interlayer water in the form of a 10 Å kaolinite hydrate.

The application of Raman microscopy to the study of intercalated kaolinites has proven most useful.[18−20] An additional Raman band, attributed to the inner-surface hydroxyl groups strongly hydrogen bonded to the acetate, was observed at 3605 cm^{-1} for the potassium acetate intercalate with the concomitant loss of intensity in the bands at 3652, 3670, 3684, and 3693 cm^{-1}. Intercalation of halloysite resulted in a Raman pattern similar to that of an intercalated ordered kaolinite. Thus the intercalated halloysite resembled the intercalated kaolinite, at least on a molecular level.[20] Here the conclusion was made

* Author to whom correspondence should be addressed.
† Queensland University of Technology.
‡ University of Veszprem.

10.1021/jp982035f CCC: $15.00
Published on Web 10/01/1998

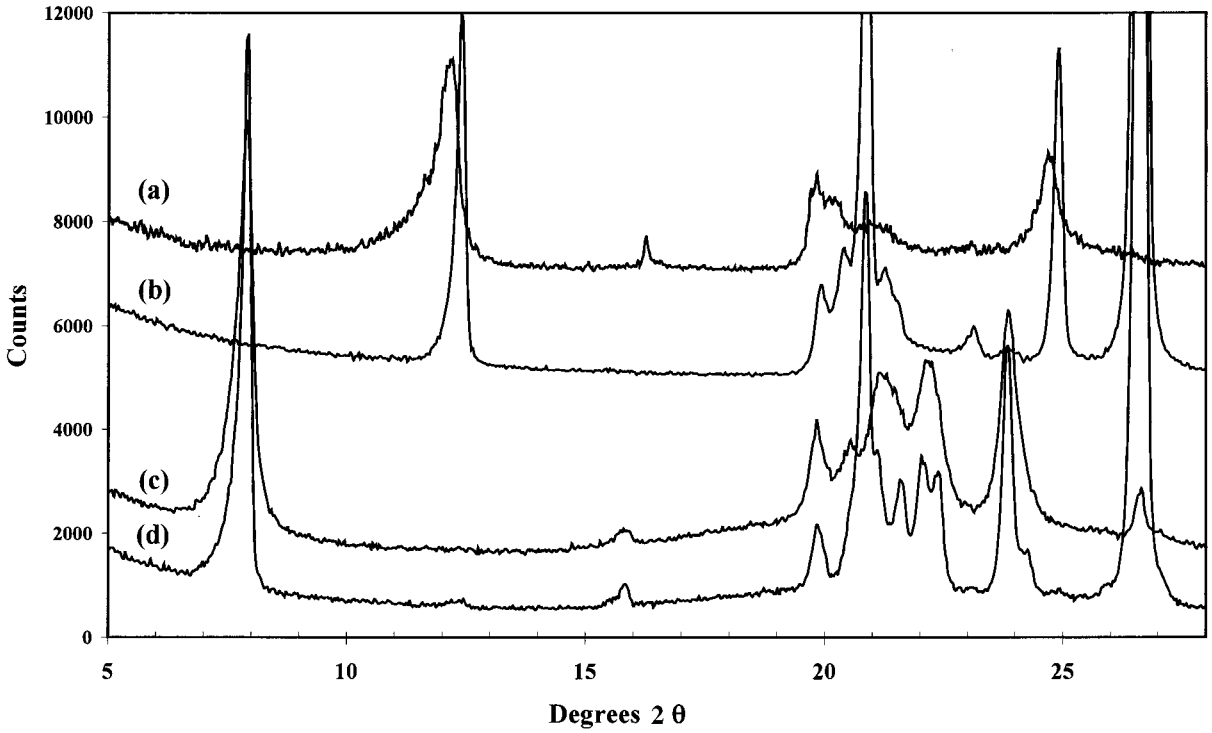

Figure 1. X-ray diffraction of (a) high-defect kaolinite, (b) low-defect kaolinite, (c) DMSO intercalated high-defect kaolinite, and (d) DMSO intercalated low-defect kaolinite.

that the intercalation process resulted in a decrease in the defect structures of the kaolinite. Remarkable changes in intensity of the Raman spectral bands of the low-frequency region of the kaolinite also occurred upon intercalation. In particular, the 935 cm^{-1} band increased in intensity upon intercalation. On the basis of the above examples, it can be concluded that Raman spectroscopy has proven most suitable for the spectroscopic analysis of intercalated kaolinites. In this paper we report the changes in the molecular structure of both a low- and high-defect kaolinite intercalated with DMSO.

Experimental Section

Intercalation of Kaolinites. The kaolinites used in this study were from Kiralyhegy and Szeg in Hungary. The first kaolinite is an example of an ordered kaolinite, and the second of a disordered kaolinite.[19−20] These kaolinites were intercalated by mixing 1 g of the kaolinite in anhydrous DMSO in an ampule, which was sealed under nitrogen and kept at 85 °C for 7 days. Raman spectra show the presence of water in the so-called pure, anhydrous DMSO. It should be noted that in the preparation of the DMSO−kaolinite intercalate by previous workers, water−DMSO mixtures were used.[22−24] In fact, Olejnik found that the optimum rate of intercalation occurred when the kaolinite was suspended in DMSO containing 9% water.[21]

X-ray Diffraction. XRD analyses were carried out on a Philips wide angle PW 1050/25 vertical goniometer equipped with a graphite diffracted beam monochromator. The *d* spacing and intensity measurements were improved by application of a self-developed computer-aided divergence slit system enabling constant sampling area irradiation (20 mm long) at any angle of incidence. The goniometer radius was enlarged from 173 to 204 mm. The radiation applied was CuKα from a long, fine-focus Cu tube, operating at 40 kV and 40 mA. The samples were measured at 50% relative humidity in step-scan mode with steps of 0.02° 2θ and a counting time of 2 s. Measured data were corrected with the Lorentz polarization factor (for oriented specimens) and for their irradiated volume.

Spectroscopy. Very small amounts of the kaolinite or the intercalated clay mineral were placed on a polished metal surface on the stage of an Olympus BHSM microscope, equipped with 10x, 20x, and 50x objectives. The microscope is part of a Renishaw 1000 Raman microscope system, which also includes a monochromator, a filter system, and a charge-coupled device (CCD). Raman spectra were excited by a Spectra-Physics model 127 He/Ne laser (633 nm) and recorded at a resolution of 2 cm^{-1} and were acquired in sections of approximately 1000 cm^{-1} for 633 nm excitation. Repeated acquisitions using the highest magnification were accumulated to improve the signal-to-noise ratio. Spectra were calibrated using the 520.5 cm^{-1} line of a silicon wafer. The best method of placing the kaolinites on this metal surface was to take a very small amount on the end of the spatula and then tap the crystals onto the metal surface. Further details on the spectroscopy have been published elsewhere.[24−26]

Diffuse reflectance Fourier transform infrared spectroscopy (commonly known as DRIFT) analyses were undertaken using a Bio-Rad 60A spectrometer. A total of 512 scans were obtained at a resolution of 2 cm^{-1}. Spectral manipulation such as baseline adjustment, smoothing, and normalization was performed using the Spectracalc software package GRAMS (Galactic Industries Corporation, NH). Band component analysis was undertaken using the Jandel Peakfit software package which enabled the type of fitting function to be selected and allows specific parameters to be fixed or varied accordingly. Band fitting was done using a Lorentz−Gauss cross-product function with the minimum number of component bands used for the fitting process. The Gauss−Lorentz ratio was maintained at values greater than 0.7, and fitting was undertaken until reproducible results were obtained with squared correlations of r^2 greater than 0.995.

Results and Discussion

X-ray Diffraction. Figure 1 shows the X-ray diffraction patterns of the low-defect and high-defect kaolinites and their

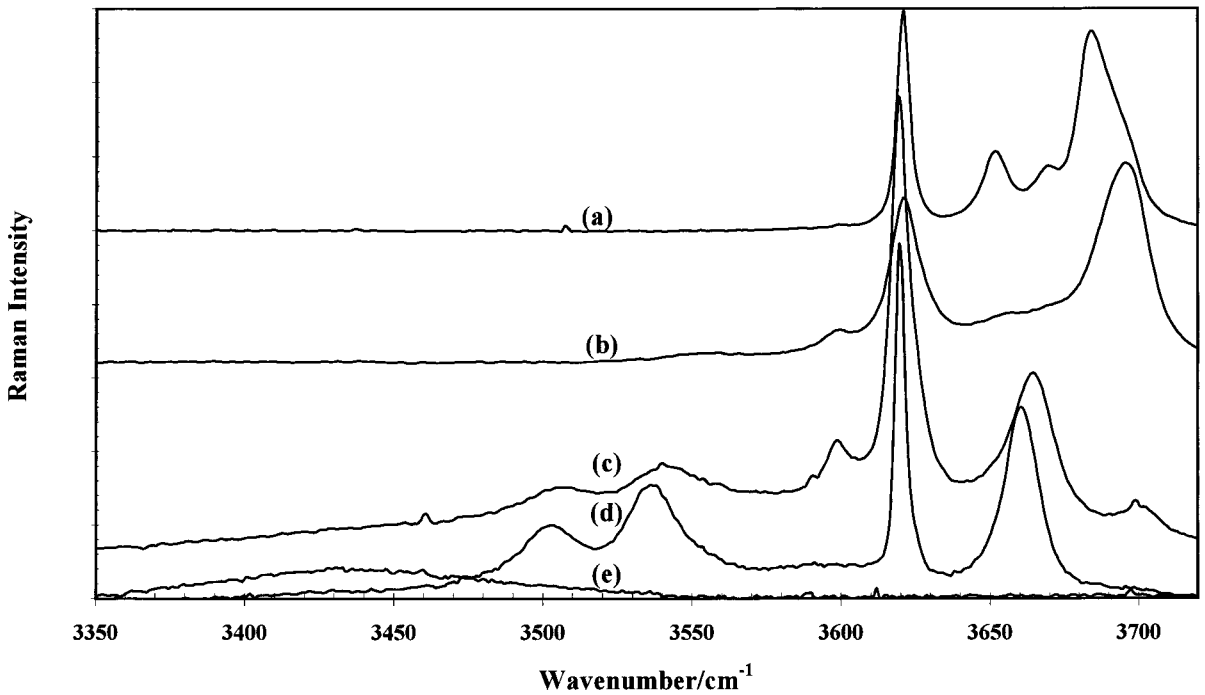

Figure 2. Raman spectra of the hydroxyl stretching region of (a) low-defect kaolinite, (b) high-defect kaolinite, (c) DMSO intercalated high-defect kaolinite, (d) DMSO intercalated low-defect kaolinite, and (e) DMSO.

DMSO intercalates. X-ray diffraction shows that the kaolinites are intercalated to the 98% level. Both kaolinites show a shift of the 001 reflection from 7.16 to 11.19 Å. Additionally, an increase in the background in the 15 to 30 degrees 2θ has occurred with a broad band centered at ~22 degrees 2θ. The significance of this broad band is that the two intercalated kaolinites are now showing a certain degree of amorphicity. The intensity of this broad band would indicate that ~30% of the kaolinites are now amorphous. An alternative proposal is based on two types of DMSO intercalated kaolinites in the intercalate, namely a single-layer kaolinite and a multidimensional DMSO intercalated kaolinite. In the case of a single-layer kaolinite, the DMSO would simply be adsorbed on the surface. The kaolinite expands from 7.16 to 11.19 Å. This is an increase of 4.03 Å. The size of the S═O group is 3.38 Å, and if the DMSO is parallel to the siloxane surface then there is an imbalance of 0.67 Å. The question arises as to how this gap may be filled. In the model of the DMSO−kaolinite intercalate presented by Thompson and Cuff, one of the methyl groups is pointing directly into the ditrigonal cavity with the second methyl group pointing away from this surface.[9] The oxygen of the S═O group is pointing toward two or three of the inner-surface hydroxyls. This model, however, is based on an absence of water in the intercalate and also depends on the presence of nonpolymeric DMSO. Scherer calculations show that the low-defect kaolinite had 52 layers stacked in the crystals, and after intercalation with DMSO this was reduced to 33 layers. For the high-defect kaolinite, the untreated kaolinite has 17 layers, and after intercalation there were 19 layers in the crystal. Taking into account the accuracy of the calculation it is assumed that the number of layers in the crystal did not change for the high-defect kaolinite. The significance of the reduction of the Scherer number for the low-defect kaolinite is that the DMSO molecules are peeling off the layers of the kaolinite as intercalation proceeds.

Hydroxyl Stretching. The Raman spectra of the hydroxyl-stretching region of the low- and high-defect kaolinites and the low- and high-defect DMSO intercalated kaolinites together with DMSO are shown in Figure 2. New Raman bands formed as a result of the DMSO intercalation are observed at 3660, 3536, and 3501 cm^{-1} for the low-defect kaolinite. It should be noted that the Raman spectrum of the DMSO contains water, as evidenced by the broad band at 3430 cm^{-1}. Further water is not easily observed in the Raman spectrum. The results of the band component analyses of the Raman spectrum of the hydroxyl-stretching region are reported in Table 1. The bandwidths (as fwhh) of the 3660, 3536, and 3501 cm^{-1} bands are 13.0, 19.0, and 24.0 cm^{-1}, respectively. The relative intensities of these bands are 34.0, 21.5, and 23.5% of the total

TABLE 1: Band Positions, Half Widths, and Band Areas of the Raman Spectrum of the Hydroxyl Stretching Region of (a) Kaolinite, (b) Low-Defect Kaolinite Intercalated with DMSO, (c) High-Defect Kaolinite Intercalated with DMSO

sample	band center (cm^{-1})	band widths (cm^{-1})	% area
Hydroxyl Stretching Region of Ordered Kaolinite			
ν_1	3693	15.2	17.7
ν_4	3684	9.5	30.0
ν_2	3670	15.4	15.4
ν_3	3651	11.5	14.5
ν_5	3620	5.7	20.8
Hydroxyl Stretching Region of Low-Defect Kaolinite Intercalated with DMSO			
ν_1	not observed		
ν_4	not observed		
ν_2	3660	13.0	34.0
ν_3	not observed		
ν_5	3620	3.7	21.0
ν_6	3536	19.0	21.5
ν_7	3501	24.0	23.5
Hydroxyl Stretching Region of High-Defect Kaolinite Intercalated with DMSO			
ν_1	3700	12.2	1.7
ν_4	not observed		
ν_2	3664	17.0	18.0
ν_3	not observed		
ν_5	3620	8.1	25.0
ν_6	3598	9.0	2.0
ν_7	3543	21.0	3.3
ν_8	3509	29.0	22.0

area of the band profile. No intensity remained in the ν_1 to ν_4 modes. The absence of intensity in these Raman bands suggests that the low-defect kaolinite was fully intercalated. Upon intercalation of the high-defect kaolinite, bands were observed at 3664, 3598, 3543, and 3509 cm^{-1}. The bands are broad with bandwidths of 17.0, 9.0, 21.0, and 29.0 cm^{-1}, respectively. These bands appear at slightly higher frequencies than those of the low-defect kaolinite. These bands make up 18.0, 2.0, 3.3, and 22% of the total band intensity. For the high-defect kaolinite, significant intensity remains in the 3700 cm^{-1} band. This band is attributed to nonsymmetric hydrogen bonding between the inner-surface hydroxyl groups and the siloxane layer.[25] It is proposed that the high-defect kaolinite was not fully intercalated as a result of the disorder which prevented the full intercalation of this kaolinite with DMSO.

It should be noted that another band also occurs at 3598 cm^{-1} for the high-defect kaolinites intercalated with DMSO. Such a band was not observed for the low-defect kaolinites intercalated with DMSO. The band was also absent in the Raman spectra of the DMSO intercalated ordered kaolinite from Georgia.[22] It has been suggested that the FTIR equivalent of this band is attributable to the hydroxyl stretching frequency of the inner hydroxyl group; this assignment seems unlikely.[27] The shift of the inner-surface hydroxyl frequency is simply too large to be plausible. Also this band is not present for all DMSO intercalated kaolinites. A more likely conclusion is that the band is due to water associated with the hydration of the kaolinite layers. It should be noted that the DMSO intercalated kaolinites were prepared using pure and dry DMSO. The absence of water was maintained throughout the experiment. Nevertheless, differential thermogravimetric analysis (DTGA) shows the presence of 7% water in the intercalated complex. Garcia and Camazano showed that DMSO−kaolinite intercalate had a tubular morphology similar to that of an halloysite.[1] Bands in similar positions are sometimes observed in the Raman spectra of halloysites. Yariv reported bands in similar positions and assigned these bands to inner-surface hydroxyls perturbed by interlamellar water.[28] However such a band may be easily described as the hydroxyls of non-hydrogen bonded interlamellar water. Further water bands have been observed at this frequency for sepiolites and attapulgites.[29] The bandwidth of the 3598 cm^{-1} band is 9.0 cm^{-1}, which is narrow for a band due to water hydroxyls. However, if the water was free of hydrogen bonding as would be expected for this frequency, then a narrow bandwidth is feasible.

The bandwidth of the 3536 and 3501 cm^{-1} bands for the low-defect kaolinite intercalated with DMSO are 19.0 and 24.0 cm^{-1}. These bands are very broad compared with the bandwidths of the kaolinite hydroxyl stretching frequencies and are assigned to the OHs of water in the DMSO intercalated kaolinite. These two bands occur at slightly different frequencies for the high-defect kaolinite and are observed at 3543 and 3509 cm^{-1}. The widths of these two bands are 21.0 and 29.0 cm^{-1}. It is hypothesized that water plays a significant role in the intercalation of the DMSO. The question might be asked as to the origin of the water and the answer lies with the DMSO itself, which does contain some water as may be observed by the spectrum in Figure 2e. Simultaneous DTA−TGA−TGMS of the DMSO intercalated kaolinite shows a complex pattern. Three endotherms are observed at 70, 113, and 168 °C. At 70 °C, water loss is observed. At 113 and 168 °C, DMSO is lost. Thus two different types of DMSO molecules are observed in the intercalates. Dehydroxylation occurs between 420 and 630 °C with the main TGA peak occurring at 540 °C. DTGA shows the presence of 7% water in the intercalate. It is probable that the three endotherms correspond to the three water Raman hydroxyl bands. Indeed, it is proposed that the water molecule is essential for the intercalation process with DMSO to occur. It is proposed that the water hydrates the siloxane layer. Indeed, this is why deintercalation of the DMSO intercalated kaolinite results in the formation of hydrated kaolinites.[15−17]

The bandwidth of the inner hydroxyl group at 3620 cm^{-1} is 5.7 cm^{-1} for the untreated kaolinite but is now 3.7 cm^{-1} for the DMSO intercalated low-defect kaolinite. Such a decrease in bandwidth is remarkable. Such a result suggests that the inner hydroxyl group is becoming better defined in its position in the kaolinite structure. The significance of this decrease rests with the positioning of the S═O of the DMSO molecule. If the DMSO molecule inserts into the ditrigonal cavity of the siloxane layer, through the S═O group, the polarity of the S═O group may well affect the polarizability of the inner hydroxyl group. Such a concept was hypothesised by Johnston.[22] For the high-defect kaolinite the width of the inner hydroxyl group is broad with a bandwidth of 7.9 cm^{-1}, and upon intercalation a bandwidth of 8.1 cm^{-1} is observed. The conclusion may be made that there is little change for the high-defect kaolinite. It is proposed that the DMSO intercalation of kaolinite depends on the defect structure of the kaolinite. Ordered kaolinites intercalate more easily with DMSO than disordered kaolinites. The reason for this is that the DMSO takes on a well-defined structure within the kaolinite lattice. The disordered kaolinite prevents this well-defined structure from occurring.

DRIFT spectroscopy shows new bands for low-defect kaolinite intercalated with DMSO at 3660, 3538, and 3502 cm^{-1}. Figure 3 shows the DRIFT spectra of the low-defect kaolinite intercalated with DMSO. Table 2 reports the band component analyses of the DRIFT spectra of the low- and high-defect kaolinites intercalated with DMSO. These values are in close agreement with the results from Raman spectroscopy. Bands in similar positions have been reported using attenuated total reflectance techniques.[8] These bands have been previously assigned to the inner-surface hydroxyl groups hydrogen bonded to the S═O of the DMSO. The ν_4 mode is not observed in the FTIR spectra, as it is infrared-inactive. No bands at ∼3670 and 3650 cm^{-1} were observed. The intensity of the ν_1 band was only 0.9%. This low value suggests the low-defect kaolinite was fully intercalated. Spectra reported previously show strong intensities in the bands of this region.[8,21−22] In these works, the kaolinites were only partially intercalated. Bands are observed at 3538 and 3502 cm^{-1} for the low-defect kaolinite with bandwidths of 25.0 and 29.0 cm^{-1}, respectively. These bands are observed at 3539 and 3504 cm^{-1} for the high-defect kaolinite with bandwidths of 27.7 and 39.4 cm^{-1}. The widths of these bands again suggest that these bands are attributable to water in the intercalation complex. It is difficult to understand why there should be three different OH frequencies (at 3660, 3538, and 3502 cm^{-1}) with such a wide difference in band position, as can be described as hydrogen bond formation between the inner-surface hydroxyls and the S═O group. In this paper, we consider that the 3660 cm^{-1} band is the result of the hydrogen bond formation of the S═O group and the inner-surface hydroxyls. The other two bands are from water which is incorporated into the DMSO intercalate structure. A band of low intensity was observed for the high-defect kaolinite at 3599 cm^{-1} with a bandwidth of 9.5 cm^{-1}. This band, attributed to interlamellar water, is not observed in the DRIFT spectrum of the low-defect kaolinite, intercalated with DMSO. In the DRIFT spectrum of the DMSO intercalated low-defect kaolinite

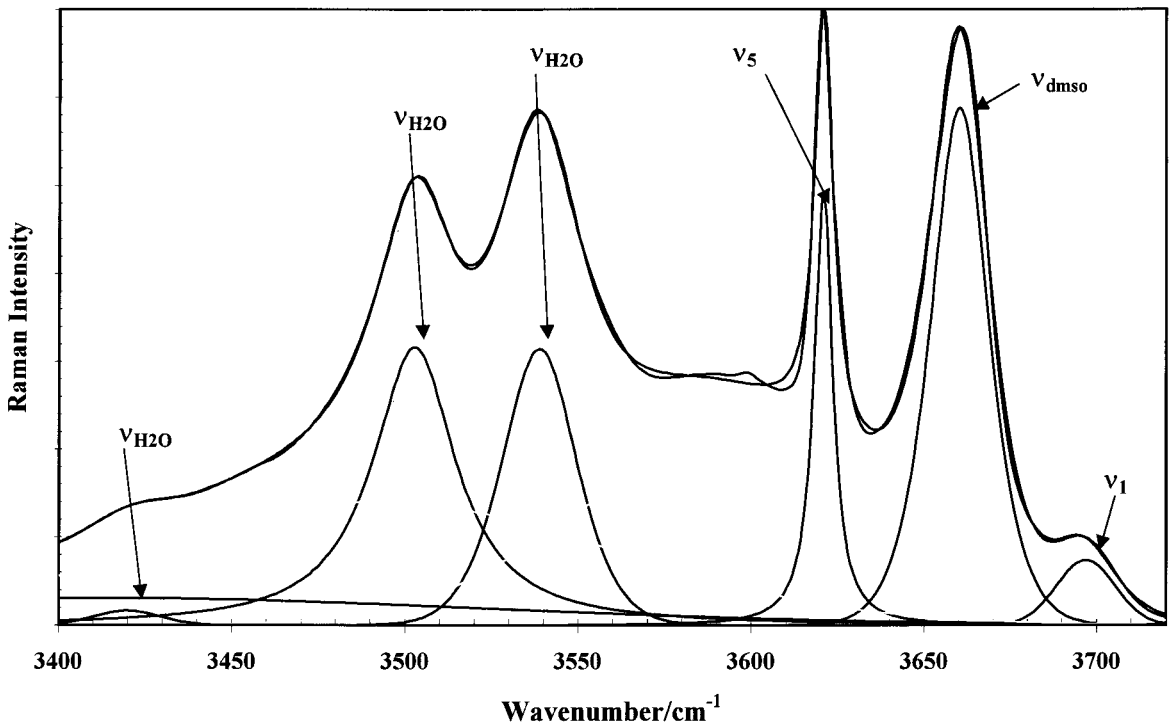

Figure 3. Band component analysis of the DRIFT spectrum of the hydroxyl stretching region of DMSO intercalated low-defect kaolinite.

TABLE 2: Band Positions, Half Widths, and Band Areas of the Infrared Spectrum of the Hydroxyl Stretching Region of (a) Low-Defect Kaolinite Intercalated with DMSO and (b) High-Defect Kaolinite Intercalated with DMSO

sample	band center (cm^{-1})	band widths (cm^{-1})	% area
DRIFT Spectrum of the Hydroxyl Stretching Region of Low-Defect Kaolinite Intercalated with DMSO			
ν_1	3697	20.0	0.9
ν_4	not observed		
ν_2	3660	19.8	7.3
ν_3	not observed		
ν_5	3620	6.5	5.2
ν_6	3538	25.0	9.6
ν_7	3502	29.0	14.6
ν_8	3492	broad	25.9
ν_9	3413	broad	9.3
DRIFT Spectrum of the Hydroxyl Stretching Region of High-Defect Kaolinite Intercalated with DMSO			
ν_1	3700	18.7	1.1
ν_4	not observed		
ν_2	3663	29.4	9.9
ν_3	not observed		
ν_5	3620.6	14.6	3.3
ν_6	3599	9.5	0.3
ν_7	3558	21.4	0.3
ν_8	3539	27.7	2.5
ν_9	3504	39.4	4.4
ν_{10}	3468	broad	39.6

an additional band was observed at 3423 cm^{-1}. This band is attributed to water which is coordinated to the S═O group of the DMSO. The band makes up 1.5% of the total band profile. This band was not observed in the DRIFT spectrum of the high-defect kaolinite.

Hydroxyl Deformation. Figure 4 illustrates the Raman spectrum of the hydroxyl deformation region of (a) DMSO, (b) DMSO intercalated low-defect kaolinite, and (c) DMSO intercalated high-defect kaolinite. The Raman spectrum of the hydroxyl deformation region of the DMSO intercalated low-defect kaolinite is characterized by three major bands at 959, 941, and 905 cm^{-1} with two minor components at 923 and 913 cm^{-1} (Figure 5). The relative intensities of the first three bands are 38.4, 25.0, and 27.0% of the total band intensity of this region. The results of the band component analyses are summarized in Table 3. For the untreated kaolinite, three bands which are assigned to the inner-surface hydroxyls are observed at 957, 935, and 923 cm^{-1} with relative intensities of 9.0, 28.5, and 15.9%. The two minor components make up 1.5 and 7.2%. The band at 959 cm^{-1} is assigned to a DMSO symmetric methyl-rocking mode.[29] The band occurs at 953 cm^{-1} for the pure liquid DMSO and moves to the higher frequency of 959 cm^{-1} upon intercalation. The increase in the frequency of this band upon intercalation is attributed to the interaction between the methyl groups and the siloxane surface. The band at 941 cm^{-1} is attributed to the hydroxyl deformation of the inner-surface hydroxyls. It is not possible to separate the contribution of the 940 cm^{-1} band of the untreated kaolinite as this band overlaps with the DMSO methyl-rocking band. Nevertheless the intercalation of the kaolinite with DMSO caused significant differences in the intensities of the bands at 941 and 923 cm^{-1}.

Intercalation of the kaolinite with DMSO has caused the rearrangement of the orientation of the kaolinite hydroxyls such that different hydroxyl deformation modes are observed. In particular, the band at 905 cm^{-1} is attributed to the hydroxyl deformation of the inner-surface hydroxyl groups which are hydrogen bonded to the S═O group of the DMSO. The DRIFT spectra of the hydroxyl deformation region of the low-defect kaolinite intercalated with DMSO shows basically two bands at 958 and 906 cm^{-1} with a minor components at 940 cm^{-1}. The areas of the 958 and 906 cm^{-1} bands are 83.7 and 15.2%. The minor components at 940 cm^{-1} make up 1.0% of the total band area. A single intense band at the 906 cm^{-1} position with a bandwidth of 16.2 cm^{-1} dominates the band profile. The band profile can be fitted with components centered at 915 and 923 cm^{-1}. However, the fit is not good (r^2 is ~0.935), and therefore the information is not included in Table 3. This DRIFT band is attributed to the hydroxyl deformation mode of the inner-surface hydroxyls hydrogen bonded to the S═O unit of the DMSO. Upon intercalation of the high-defect kaolinite with DMSO, hydroxyl deformation bands in the Raman spectrum

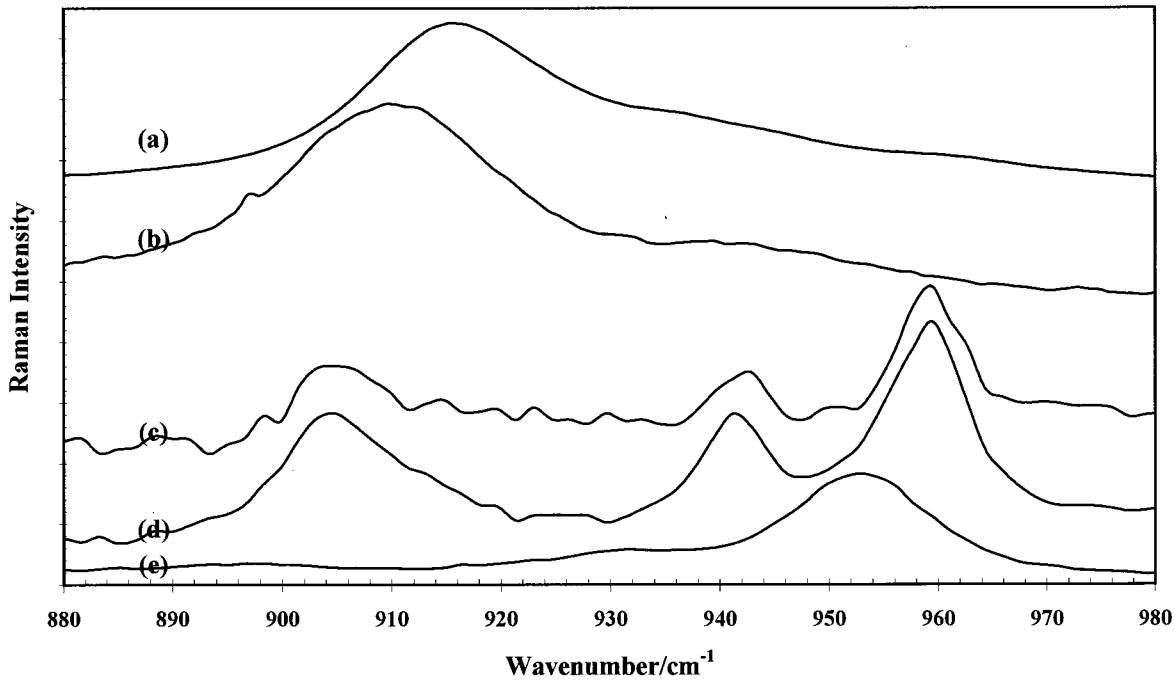

Figure 4. Raman spectra of the hydroxyl deformation region of (a) DMSO, (b) DMSO intercalated low-defect kaolinite, and (c) DMSO intercalated high-defect kaolinite.

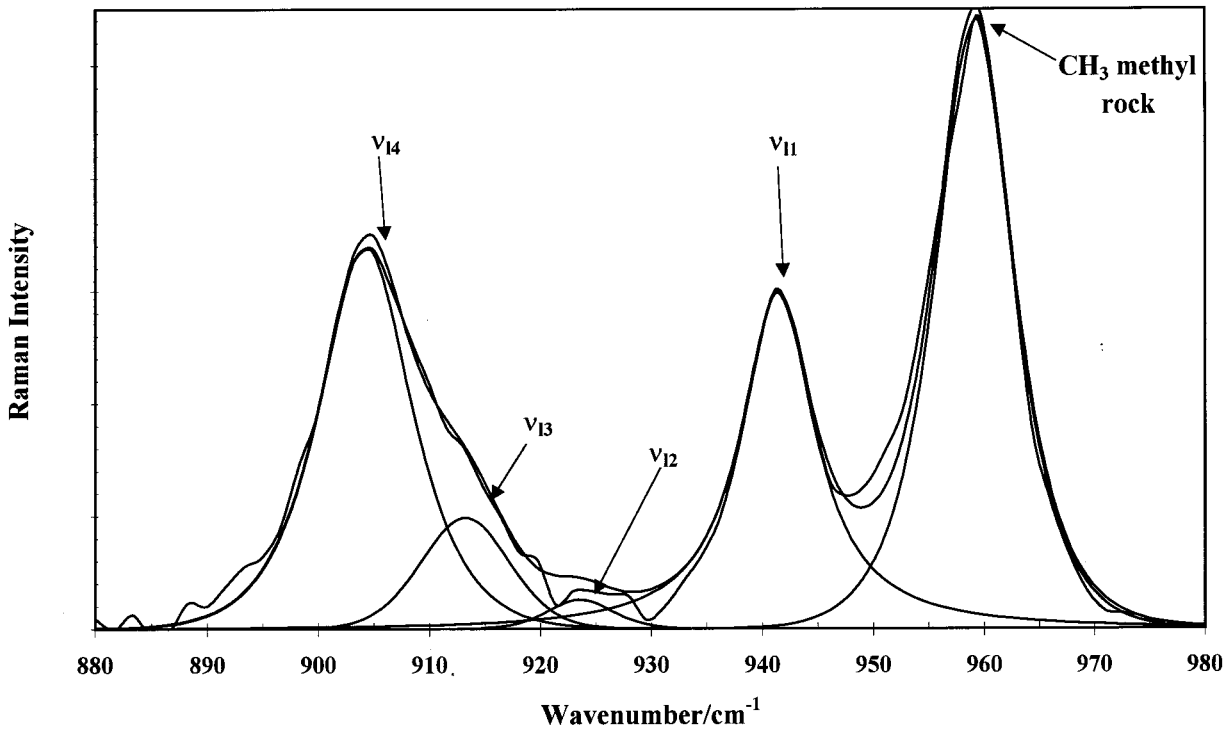

Figure 5. Band component analysis of the Raman spectrum of the hydroxyl deformation region of DMSO intercalated high-defect kaolinite.

are observed at 942, 923, 913, and 905 cm^{-1}. This spectral region is dominated by the 959 cm^{-1} peak that makes up 42% of the total intensity. The peak at 905 cm^{-1} makes up 24% of the total intensity. Some intensity remains in the 942 and 913 cm^{-1} bands, and these bands are attributed to the hydroxyl deformation modes of the inner-surface hydroxyl that was not hydrogen bonded to the DMSO and to the inner hydroxyl group. The DRIFT spectra of this region for the DMSO intercalated low-defect kaolinite are dominated by the band at 906 cm^{-1} which makes up 83.7% of the total band intensity. The equivalent band for the high-defect kaolinite occurs at 904 cm^{-1} and has a relative intensity of 71%.

If the DMSO kaolinite intercalate had three different OH stretching frequencies which were attributed to the hydrogen bonding of the inner-surface hydroxyls to the S═O of the DMSO, then it could be expected that three different hydroxyl deformation modes would be observed. This is not observed. Rather one single intense band centered at 905 cm^{-1} is observed. This observation suggests that only one type of hydrogen bonded inner-surface hydroxyl group is formed. In the DRIFT spectra of the DMSO intercalated low-defect kaolinite, two water bending vibrations are observed at 1610 and 1683 cm^{-1} with areas of 66 and 33%. The bandwidths of these bands were 39.9 and 45.9 cm^{-1}. These two water bending modes show that two

TABLE 3: Band Positions, Half Widths, and Band Areas of the Raman and DRIFT Spectra of the Hydroxyl Deformation Region of (a) Kaolinite, (b) Low-Defect Kaolinite Intercalated with DMSO, and (c) High-Defect Kaolinite Intercalated with DMSO

sample	band center (cm^{-1})	band widths (cm^{-1})	% area
Raman Spectrum of the Hydroxyl Deformation Region of Ordered Kaolinite			
ν_{I1}	957	19.4	9.0
ν_{I2}	935	22.5	28.5
ν_{I3}	923	19.1	15.9
ν_{I4}	915	19.1	58.5
Raman Spectrum of the Hydroxyl Deformation Region of Low-Defect Kaolinite Intercalated with DMSO			
DMSO	959	8.2	38.4
ν_{I1}	941	8.0	25.0
ν_{I2}	923	6.9	1.5
ν_{I3}	913	9.3	7.2
ν_{I4}	905	9.7	27.0
Raman Spectrum of the Hydroxyl Stretching Region of High-Defect Kaolinite Intercalated with DMSO			
DMSO	959	8.2	42.0
ν_{I1}	942	9.0	15.0
ν_{I2}	923	7.3	1.5
ν_{I3}	913	8.9	9.6
ν_{I4}	905	10.0	24.0
DRIFT Spectrum of the Hydroxyl Stretching Region of Low-Defect Kaolinite Intercalated with DMSO			
ν_{I1}	958	6.7	15.2
ν_{I2}	940	4.5	1.0
ν_{I3}	906	16.2	83.7
ν_{I5}	not observed		
DRIFT Spectrum of the Hydroxyl Stretching Region of High-Defect Kaolinite Intercalated with DMSO			
ν_{I1}	958	8.0	6.4
ν_{I2}	943	22.2	4.4
ν_{I3}	904	24.0	71.0
ν_{I5}	869	22.5	18.3

different types of water molecules are present. For the disordered kaolinite an additional band is also found at 1583 cm^{-1}.

Adsorbed water gives strong infrared bands at 3450 cm^{-1}, the water hydroxyl stretching vibration, and at $\sim$ 1630 cm^{-1}, the water bending vibrations. For monomeric non-hydrogen bonded water as occurs in the vapor phase, these bands are found at 3755 and 1595 cm^{-1}. For liquid water the bands occur at 3455 and 1645 cm^{-1}, and for water molecules in ice the bands are at 3255 and 1655 cm^{-1}.[29] The hydroxyl stretching modes of weak hydrogen bonded water molecules occur in the 3590 to 3500 cm^{-1} region, and the hydroxyl stretching modes of strong hydrogen bonds occur below 3420 cm^{-1}. When the water is coordinated to the cation in clays, as occurs in certain minerals such as hisingerite and palygorskites,[29] the water OH stretching frequency occurs at 3220 cm^{-1}. A simple observation can be made that as the water OH stretching frequency decreases, the HOH bending frequency increases. The 3220 cm^{-1} band corresponds to an ice-like structure with O−H···O bond distances of 2.77 Å. Thus the water hydroxyl stretching and the water HOH bending frequencies provide a measure of the strength of the bonding of the water molecules either chemically or physically to the clay minerals. Bands that occur at frequencies above 1650 cm^{-1} are indicative of coordinated water and chemically bonded water. Bands that occur below 1630 cm^{-1} are indicative of water molecules that are not as tightly bound. In the case of kaolinite intercalated with DMSO, two types of water are present: (1) weakly hydrogen bonded water, and (2) coordinated water. The band at 1683 cm^{-1} is attributed to strongly hydrogen bonded water. It is proposed that this water is coordinated to the DMSO molecule and may act as the linking molecule in joining several DMSO molecules in a polymer. Upon deintercalation of the DMSO intercalated kaolinite this water is then retained to form a hydrated kaolinite.[16,17] It is probable that the hydroxyl stretching frequency at 3501 cm^{-1} is associated with the 1683 cm^{-1} bending mode. It is suggested that this water is water that is hydrogen bonded to the DMSO molecules. The band at 3536 cm^{-1} is associated with the 1610 cm^{-1} hydroxyl deformation frequency. These bands are attributed to adsorbed water. For the high-defect kaolinite, the additional band at 3598 cm^{-1} is associated with the hydroxyl deformation frequency at 1583 cm^{-1}. These bands are assigned to water that is non-hydrogen bonded water which is filling spaces in the expanded lattice. These bands are found only for disordered DMSO intercalates and are not observed for the low-defect DMSO intercalated kaolinites. Thus these assignments support the concept that the additional bands in the Raman and infrared spectra in the 3500−3600 cm^{-1} range are associated with the presence of water in the intercalate.

Methyl Vibrations. The Raman spectra of C−H stretching region of DMSO and the DMSO intercalated kaolinites are shown in Figure 6. Details of the band component analysis of the Raman and DRIFT spectra of the C−H stretching region of DMSO, DMSO intercalated low-defect kaolinite, and DMSO intercalated high-defect kaolinite are reported in Table 4. The DMSO shows two simple Raman bands at 2911 and 2996 cm^{-1}. These bands are attributed to the symmetric and antisymmetric stretching vibrations of the C−H of the methyl group. Upon intercalation, the 2911 cm^{-1} band splits into two bands at 2917 and 2935 cm^{-1}. This splitting is attributed to a loss of degeneracy. The 2917 cm^{-1} band is the less intense of the two bands in the Raman spectra, being the symmetric stretching mode. The two bands show that there are two different methyl groups in the DMSO intercalated kaolinite, one of which is perturbed to high frequency. Such a loss of degeneracy was observed by Johnston but the spectra of Johnston show a lack of intensity in the 2935 cm^{-1} band, which may be attributed to the partial intercalation of the kaolinite.[22] The 2996 cm^{-1} band loses its degeneracy upon intercalation, and thus four bands are observed at 2998, 3015, 3021, and 3029 cm^{-1}.

The DRIFT spectrum of DMSO shows two bands at 2918 and 2935 cm^{-1}. The 2935 cm^{-1} band is more intense in the FTIR spectra. Upon intercalation of kaolinite with DMSO, the 2996 cm^{-1} band resolves into four components at 2998, 3016, 3021, and 3029 cm^{-1}. This set of data is in good agreement with the Raman data. These bands are attributed to the antisymmetric C−H stretching modes. DRIFT spectra show one band at 3021 cm^{-1} with a small shoulder at 3016 cm^{-1} for the low-defect kaolinite and 3014 cm^{-1} for the high-defect kaolinite and a second shoulder at 3029 cm^{-1}. There is also a very weak FTIR band at 2998 cm^{-1}. This particular band is infrared-inactive Raman-active which suggests a symmetric vibration. The loss of degeneracy into four bands indicates four different asymmetric C−H stretching vibrations. Raupach[8] showed only two FTIR bands at 2936 and 3022 cm^{-1}. Johnston[22] reported two Raman bands for DMSO at 2913 and 2998 cm^{-1}, which upon intercalation split into bands at 2919 and 2936 cm^{-1} for the 2913 cm^{-1} band and into 3001, 3006, and 3116 cm^{-1} for the 2998 cm^{-1} band.[22] These results differ from the spectral data reported in this paper. The reason for this may be attributed to the fact that kaolinites in his work were not fully intercalated.

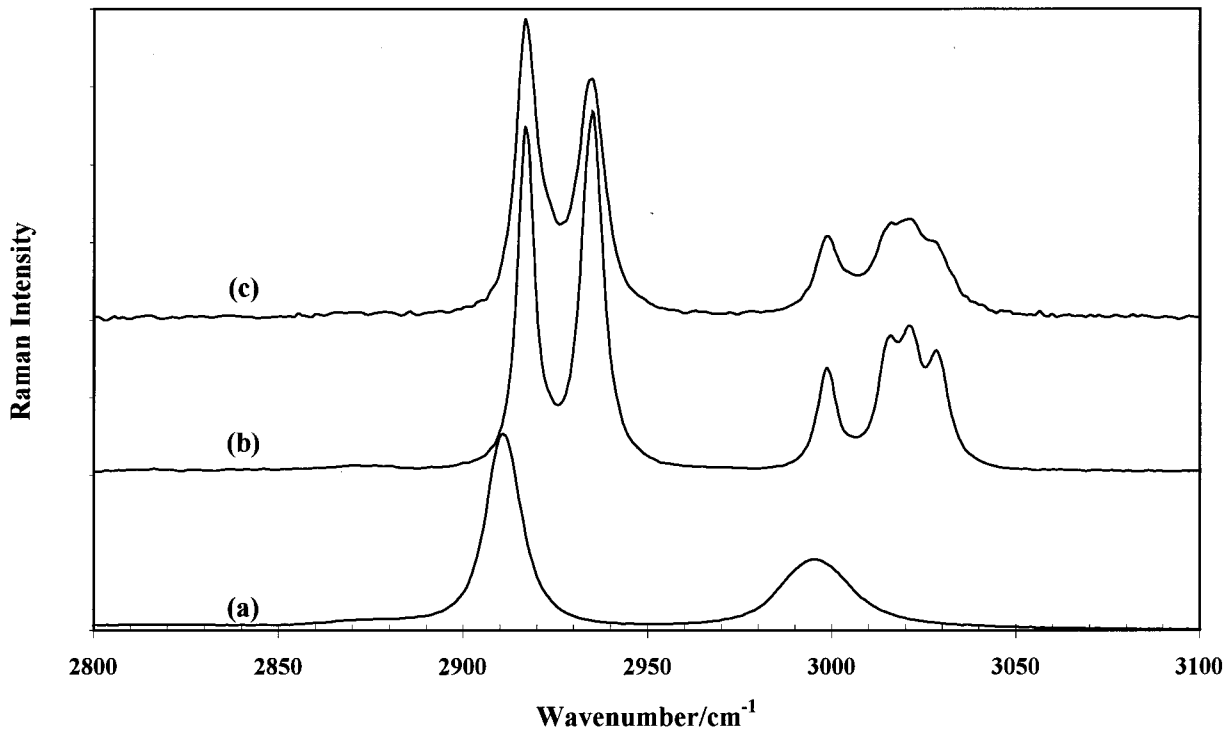

Figure 6. Raman spectra of the C−H stretching region of (a) DMSO, (b) DMSO intercalated low-defect kaolinite, and (c) DMSO intercalated high-defect kaolinite.

The bands at 2911 and 2996 cm^{-1} in the Raman spectra of pure DMSO make up 60 and 40% of the total band area and have bandwidths of 10.4 and 18.6 cm^{-1}, respectively. Upon intercalation the 2911 cm^{-1} band splits into two bands at 2917 and 2935 cm^{-1} with band areas of 27.4% and 35%. These two bands are now very sharp with bandwidths of 6.0 and 7.2 cm^{-1}, respectively. The 2996 cm^{-1} band for the DMSO methyl groups in the DMSO intercalated low-defect kaolinite splits into four bands at 2998, 3015, 3021, and 3029 cm^{-1}. These bands have areas of 9.0, 9.5, 7.2, and 11.9%, respectively, and with bandwidths of 6.7, 6.9, 7.0, and 7.5 cm^{-1}. The total area of these four bands makes up 38% of the total band area. Each of the methyl symmetric and antisymmetric stretching frequencies shows considerable band narrowing upon intercalation. The 2911 cm^{-1} band has a bandwidth of 10.4 cm^{-1} which becomes 6.0 cm^{-1} for the 2917 cm^{-1} band upon intercalation. Such bandwidths suggest that the methyl groups are held in a rigid structure. The Raman spectrum of the C−H stretching region of the DMSO intercalated high-defect kaolinite shows stretching frequencies similar to those of the low-defect intercalate. The C−H symmetric stretching frequencies are observed at 2917 and 2934 cm^{-1} with relative intensities of 31.0 and 31.8% and bandwidths of 7.3 and 9.1 cm^{-1}. These two bands are broader in the high-defect example. The total intensity of the two bands is the same for both the low- and high-defect intercalates. However, for the low-defect kaolinite the ratio of the 2917 and 2935 cm^{-1} bands is 4:5, and for the high-defect example this ratio is 1:1. Such ratios suggest that 50% of the C−H groups are in a perturbed structure and 50% are nonperturbed. It is not known whether one of the DMSO methyl groups is perturbed and the second nonperturbed, although this does seem a likely model. The antisymmetric stretching frequencies are observed at 2999, 3015, 3021, and 3028 cm^{-1}. The relative intensities of these bands are 9.8, 10.4, 3.8, and 13% and the bandwidths are 8.9, 11.0, 7.9, and 14.4 cm^{-1}. The band areas of the antisymmetric stretching modes are similar for both the low- and high-defect kaolinites. However, the widths of these

TABLE 4: Band Positions, Half Widths, and Band Areas of the Raman Spectrum of the C−H Stretching Region of (a) DMSO, (b) Low-Defect Kaolinite Intercalated with DMSO, and (c) High-Defect Kaolinite Intercalated with DMSO

sample	band center (cm^{-1})	band widths (cm^{-1})	% area
Raman Spectrum of the C−H Stretching Region of DMSO			
ν_{C-H1}	2996	18.6	39.9
ν_{C-H2}	2911	10.4	60.0
Raman Spectrum of the C−H Stretching Region of DMSO in Low-Defect Kaolinite Intercalated with DMSO			
ν_{C-H1}	3029	7.5	11.9
ν_{C-H2}	3021	7.0	7.2
ν_{C-H3}	3015	6.9	9.5
ν_{C-H4}	2998	6.7	9.0
ν_{C-H5}	2935	7.2	35.0
ν_{C-H6}	2917	6.0	27.4
Raman Spectrum of the C−H Stretching Region of DMSO in High-Defect Kaolinite Intercalated with DMSO			
ν_{C-H1}	3028	14.4	13
ν_{C-H2}	3021	7.9	3.8
ν_{C-H3}	3015	11.0	10.4
ν_{C-H4}	2999	8.9	9.8
ν_{C-H5}	2934	9.1	31.8
ν_{C-H6}	2917	7.3	31.0
DRIFT Spectrum of the C−H Stretching Region of DMSO in Low-Defect Kaolinite Intercalated with DMSO			
ν_{C-H1}	3029	6.7	7.0
ν_{C-H2}	3021	7.9	35.0
ν_{C-H3}	3016	6.5	8.0
ν_{C-H4}	2998	14.4	3.1
ν_{C-H5}	2935	7.0	32.7
ν_{C-H6}	2918	6.9	5.0
DRIFT Spectrum of the Hydroxyl Stretching Region of DMSO in High-Defect Kaolinite Intercalated with DMSO			
ν_{C-H1}	3028	14.5	13.0
ν_{C-H2}	3021	7.9	3.8
ν_{C-H3}	3014	11.0	10.4
ν_{C-H4}	2999	8.9	9.9
ν_{C-H5}	2934	9.1	31.8
ν_{C-H6}	2917	7.3	31.0
ν_{C-H7}	2906	7.0	4.3

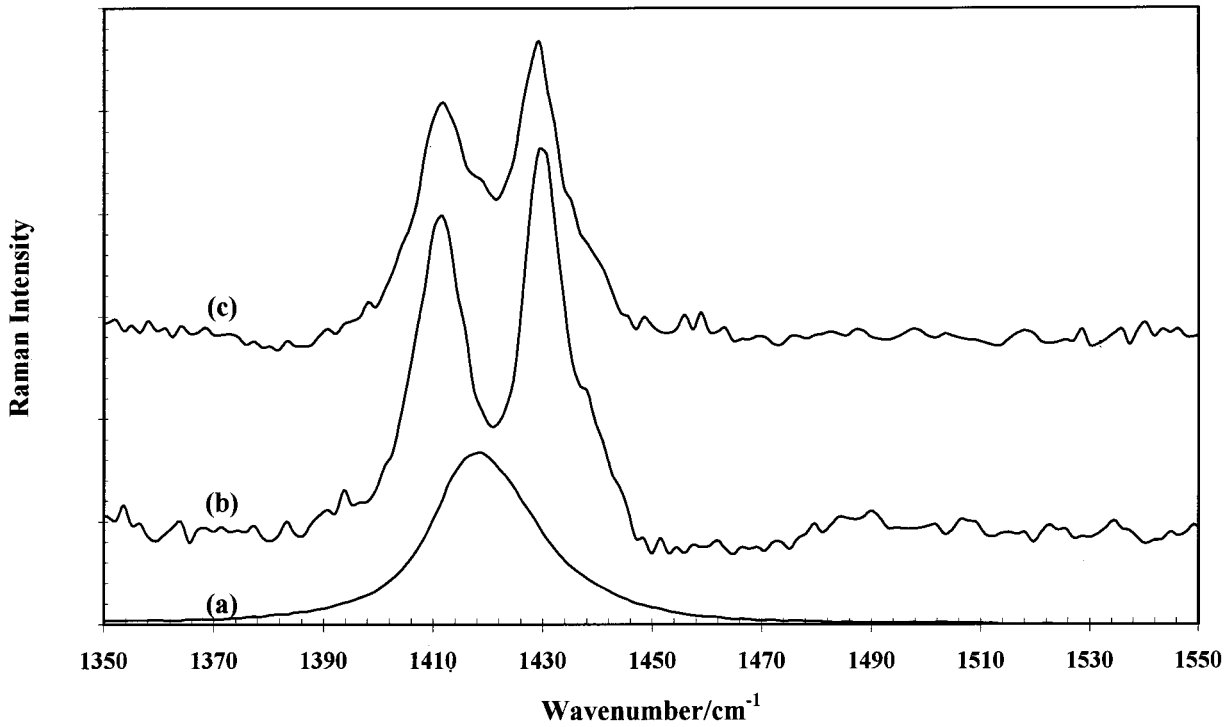

Figure 7. Raman spectra of the in-plane methyl bending region of (a) DMSO, (b) DMSO intercalated low-defect kaolinite, and (c) DMSO intercalated high-defect kaolinite.

antisymmetric stretching frequencies are considerably broader for each of the bands. The conclusion is made that the methyl groups are not in a well-defined structure for the disordered kaolinite.

For the low-defect kaolinite, the 2918 and 2935 cm^{-1} DRIFT bands make up 5.0 and 32.7% of the total normalized band area and have bandwidths of 6.9 and 7.0 cm^{-1}. As with the Raman spectra, these bands show considerable narrowing upon intercalation. Such an observation supports the concept that the DMSO molecules are being held in a crystal-like lattice. The possibility arises that the DMSO is self-coordinated rather than simply hydrogen bonded to the kaolinite. In other words, the DMSO shows some sort of polymeric behavior within the layers of the kaolinite. The bands at 3016, 3021, and 3029 cm^{-1} have also narrow bands with bandwidths of 6.5, 7.9, and 6.7 cm^{-1}. These bands make up 8.0, 35.0, and 7.0% of the total band area. The high-defect DMSO intercalated kaolinite shows C−H bands in similar positions; bands are observed at 2906, 2917, and 2934 for the C−H symmetric stretching vibration with band areas of 4.3, 31.0, and 31.8% of the total band area. These bands have bandwidths of 7.0, 7.3, and 9.1 cm^{-1}, respectively. The antisymmetric C−H stretching region shows bands at 2999, 3014, 3021, and 3028 cm^{-1} with band areas of 9.9, 10.4, 3.8, and 13%. The bandwidths of these bands are 8.9, 11, 7.9, and 14.5 cm^{-1}, respectively. Whereas for the ordered kaolinite these bands were very sharp, for the disordered kaolinites the bands are broad. Such bandwidths would imply that the intercalation of the disordered kaolinite is different from that of the ordered kaolinite. The crystal-like structure is not there for the disordered kaolinite.

The in-plane methyl bending region of the Raman spectrum shows a single band at 1419 cm^{-1} which splits into two bands at 1411 and 1430 cm^{-1} upon intercalation (Figure 7). Details of the band component analysis of the Raman and DRIFT spectra of the C−H bending region of DMSO, DMSO intercalated low-defect kaolinite, and DMSO intercalated high-defect kaolinite are reported in Table 5. The 1419 cm^{-1} band has a bandwidth of 21.9 cm^{-1}. Upon intercalation the 1411 and 1430 cm^{-1} bands have bandwidths of 10.2 and 9.2 cm^{-1}, respectively. The bands have become considerably narrower upon intercalation of the kaolinite. The DRIFT spectrum of this region for

TABLE 5: Band Positions, Half Widths, and Band Areas of the Raman Spectrum of the C−H Bending Region of (a) DMSO, (b) Low-Defect Kaolinite Intercalated with DMSO, (c) High-Defect Kaolinite Intercalated with DMSO

sample	band center (cm^{-1})	band widths (cm^{-1})	% area
Raman Spectrum of the C−H Stretching Region of DMSO			
ν_{b1}	1419	21.9	100
Raman Spectrum of the C−H Bending Region of DMSO in Low-Defect Kaolinite Intercalated with DMSO			
ν_{b1}	1430	9.2	52.2
ν_{b2}	1411	10.2	47.8
Raman Spectrum of the C−H Bending Region of DMSO in High-Defect Kaolinite Intercalated with DMSO			
ν_{b3}	1430	9.2	52.2
ν_{b4}	1411	10.2	47.8
DRIFT Spectrum of the C−H Bending Region of DMSO			
ν_{b1}	1414	16.0	45.0
ν_{b2}	1445	19.3	55.0
DRIFT Spectrum of the C−H Bending Region of DMSO in Low-Defect Kaolinite Intercalated with DMSO			
ν_{b1}	1438	11.0	10.8
ν_{b2}	1429	14.3	13.0
ν_{b3}	1427	5.4	5.3
ν_{b4}	1408	8.4	6.0
ν_{b5}	1404	23.9	25.0
ν_{b6}	1392	5.1	6.6
ν_{b7}	1373	25.4	11.4
DRIFT Spectrum of the C−H Bending Region of DMSO in High-Defect Kaolinite Intercalated with DMSO			
ν_{b1}	1438	12.3	16.2
ν_{b2}	1427	11.8	15.3
ν_{b3}	1408	16.9	13.5
ν_{b4}	1404	24.0	20.5
ν_{b5}	1392	6.0	5.5
ν_{b6}	1374	19.0	13.4

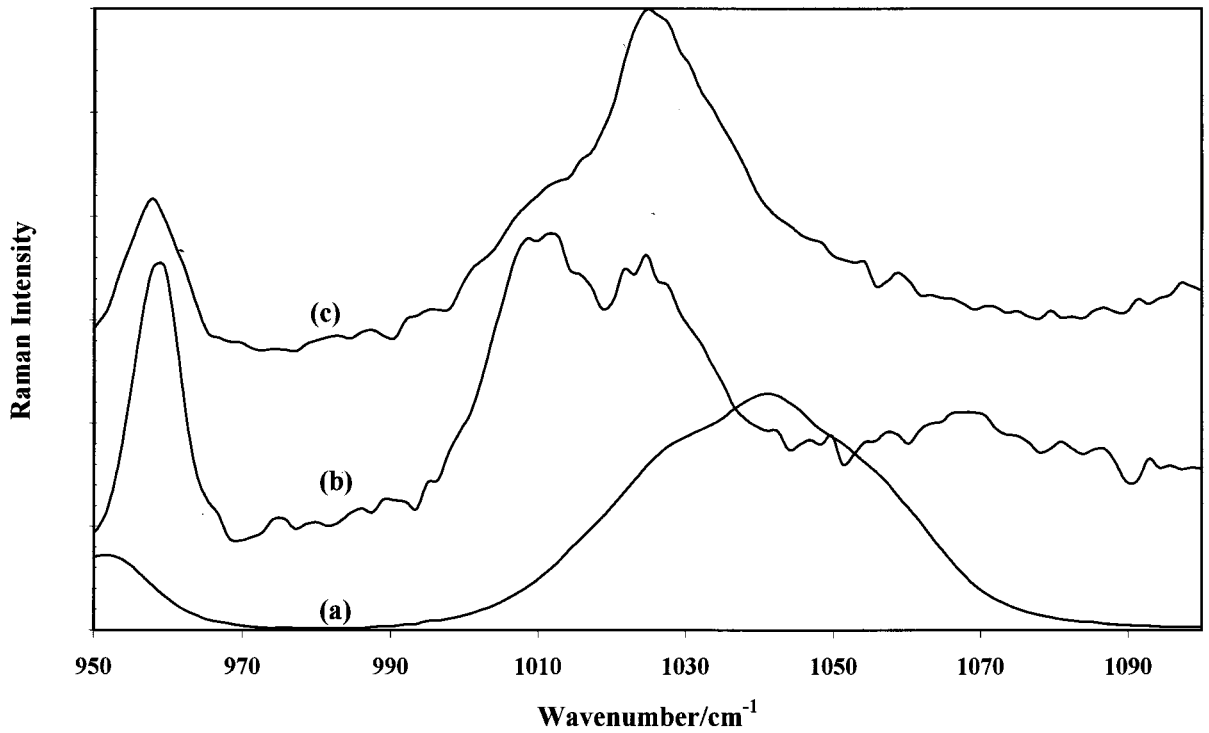

Figure 8. Raman spectra of the S═O stretching region of (a) DMSO, (b) DMSO intercalated low-defect kaolinite, and (c) DMSO intercalated high-defect kaolinite.

the DMSO intercalated low-defect kaolinite is complex with bands observed at 1438, 1428, 1408, 1404, 1392, 1374, and 1318 cm^{-1}. The DRIFT spectrum of the DMSO shows two bands at 1414 and 1445 cm^{-1}. The infrared spectrum of this region is complex. A band of low intensity is also observed at 1333 cm^{-1}. Bands are observed in similar positions for the DMSO intercalated high-defect kaolinite. This number of bands indicates at least seven different types of H−C−H bending vibrations. Infrared bands are also observed at 1317 and 1302 cm^{-1}. The complexity of the C−H bending region supports the concept of different molecular arrangements of the DMSO molecules in the intercalate.

Raman spectra of pure DMSO show bands at 1056, 1042, 1029, and 1015 cm^{-1}. These bands are attributed to S═O vibrations except for the 1015 cm^{-1} mode which is the antisymmetric methyl-rocking vibration.[30] This band splits into two bands at 1023 and 1010 cm^{-1} with bandwidths of 12.0 and 9.5 cm^{-1}, respectively, upon intercalation of the low-defect kaolinite with DMSO. The 900 to 1200 cm^{-1} DRIFT spectral region is extremely complex. The bands at 905 and 944 cm^{-1} are attributed to the hydroxyl deformation modes. The other bands are assigned to a combination of symmetric and antisymmetric S═O and methyl-rocking vibrations. Bands are observed at 1056, 1028, 1004, and 957 cm^{-1} for pure DMSO. In particular, bands are observed at 1066, 1023, and 1010 cm^{-1} for the DMSO intercalated low-defect kaolinite and at 1058, 1040, 1026, and 1010 cm^{-1} for the DMSO intercalated high-defect kaolinite.

The 1010 cm^{-1} band is attributed to antisymmetric methyl-rocking vibrations.[30] The band at 951 cm^{-1} is assigned to the symmetric methyl-rocking mode, and this band moves to 959 cm^{-1} upon intercalation of the kaolinite with DMSO (Table 3). The 8 cm^{-1} shift in frequency is accounted for by the restriction of the rocking vibration of the methyl group. This band is broad with a bandwidth of 14.4 cm^{-1} for pure DMSO and is 6.8 cm^{-1} for DMSO in the intercalate. This decrease in bandwidth indicates the methyl rocking is very rigid in its motion.

S═O Vibrational Modes. The region centered on 1040 cm^{-1} is assigned to the symmetric stretching region of S═O (Figure 8). Details of the band component analysis of the Raman and DRIFT spectra of the S═O stretching region of DMSO, DMSO intercalated low-defect kaolinite, and DMSO intercalated high-defect kaolinite are reported in Table 6. Three Raman bands are identified for pure DMSO at 1056, 1042, and 1029 cm^{-1}. These bands are assigned to the unassociated monomer, the out-of-phase and the in-phase vibrations of the dimer.[31−34] A minor component was observed at 1015 cm^{-1}. This band is normally associated with polymeric DMSO. No Raman bands which are attributable to the linear dimer and polymeric or aggregated DMSO were observed at 1027 or 1015 cm^{-1}. A band is also observed at 951 cm^{-1} which is assigned to the symmetric methyl-rocking vibration.[30] Upon intercalation of the low-defect kaolinite with DMSO, new Raman bands are observed at 1066, 1023, and 1010 cm^{-1}. For the high-defect kaolinite, bands are observed at 1058, 1040, 1026, and 1010 cm^{-1}. The two bands at 1023 and 1010 cm^{-1} are assigned to two different polymeric S═O DMSO units.[30] The broad bands at 1066 and 1058 cm^{-1} are assigned to S═O of free monomeric DMSO. Importantly, these results show that more than one type of intercalating DMSO molecule is present. For the low-defect DMSO intercalation complex, 35% of the total band intensity is in the 1066 cm^{-1} band. This suggests that 35% of the DMSO in the intercalate is present as a monomer. The loss of weight and the pronounced endotherm at 117 °C corresponds to this complex. It was observed that 37.5% of the intensity is in the 1023 cm^{-1} band. Bands for the S═O stretch of DMSO in this region are assigned to polymeric DMSO.[30−34] Therefore it is proposed that 37.5% of the DMSO is in a polymeric complex. The endotherm at 168 °C probably corresponds to the loss of this polymeric DMSO from the intercalation complex. Two bands are observed for the high-defect DMSO complex at 1058 and 1040 cm^{-1}. Both bands are attributed to monomeric DMSO, and the total band area is 38%. It was observed that 54% of the total band intensity is in the 1026 cm^{-1} band which

TABLE 6: Band Positions, Half Widths, and Band Areas of the Raman Spectrum of the S═O Stretching Region of (a) DMSO, (b) Low-Defect Kaolinite Intercalated with DMSO, (c) High-Defect Kaolinite Intercalated with DMSO

sample	band center (cm^{-1})	band widths (cm^{-1})	% area
Raman Spectrum of the S═O Stretching Region of DMSO			
$\nu_{S=O1}$	1056	19.8	19.2
$\nu_{S=O2}$	1042	20.5	34.0
$\nu_{S=O3}$	1029	28.5	37.3
$\nu_{S=O4}$	1015	19.0	7.6
Raman Spectrum of the S═O Stretching Region of DMSO in Low-Defect Kaolinite Intercalated with DMSO			
$\nu_{S=O1}$	1066	49.0	35.0
$\nu_{S=O2}$	1023	12.0	37.5
$\nu_{S=O3}$	1010	9.5	19.3
Raman Spectrum of the S═O Stretching Region of DMSO in High-Defect Kaolinite Intercalated with DMSO			
$\nu_{S=O1}$	1058	24.7	15.0
$\nu_{S=O2}$	1040	18.7	23.0
$\nu_{S=O3}$	1026	15.5	54.0
$\nu_{S=O4}$	1010	20.2	7.0
DRIFT Spectrum of the S═O Stretching Region of DMSO in Low-Defect Kaolinite Intercalated with DMSO			
$\nu_{S=O1}$	1083	18.1	2.0
$\nu_{S=O2}$	1058	21.9	5.0
$\nu_{S=O3}$	1028	44.8	20.7
$\nu_{S=O4}$	1004	32.8	13.3
$\nu_{S=O5}$	987	24.3	7.0
DRIFT Spectrum of the S═O Stretching Region of DMSO in High-Defect Kaolinite Intercalated with DMSO			
$\nu_{S=O1}$	1094	27.4	10.4
$\nu_{S=O2}$	1040	53.0	34.6
$\nu_{S=O3}$	1015	32.6	11.2
$\nu_{S=O4}$	989	45.0	10.9

is attributed to polymeric DMSO in the intercalate complex. Thus, in both the low- and high-defect DMSO intercalation complexes, two types of DMSO molecules exist. In a simple analysis, these two types of molecules may be described as polymeric and monomeric.

Figure 9 shows the 640−740 cm^{-1} spectral region. Bands are observed at 669 and 699 cm^{-1} for pure DMSO and are attributed to the symmetric and antisymmetric C−S stretching vibrations. Details of the band component analysis of the Raman spectra of the C−S stretching region of DMSO, DMSO intercalated low-defect kaolinite, and DMSO intercalated high-defect kaolinite are reported in Table 7. The areas of the 669 and 699 cm^{-1} bands are 77.0 and 23.0%, respectively, and the bandwidths are 12.6 and 15.9 cm^{-1}, respectively. The symmetric and antisymmetric C−S stretching vibrations are found at 690 and 721 cm^{-1} in the DMSO intercalated low-defect kaolinites. The area of these bands are 60.3 and 39.7% and have bandwidths of 7.2 and 5.8 cm^{-1}. The bands show symmetric profiles with only one band at each frequency for the DMSO intercalated low-defect kaolinite. The bands are substantially narrower for both the antisymmetric and symmetric C−S stretching vibrations for the DMSO intercalated low-defect kaolinite. There is a ∼21 cm^{-1} difference between the unperturbed C−S stretching frequencies and the perturbed stretching frequencies. For the high-defect kaolinite, four bands are observed at 680, 690, 720, and 712 cm^{-1}. The first two bands are assigned to the symmetric stretching modes, and the second is assigned to the antisymmetric stretching vibrations. No differences in the C−S stretching frequencies between the high-defect kaolinite and the low-defect kaolinite were found. However, a second set of bands was observed for the DMSO intercalated high-defect kaolinite at 680 and 712 cm^{-1} with bandwidths of 15.4 and 14.6 cm^{-1}, respectively. The significance of the two sets of values for both the antisymmetric and symmetric C−S stretching vibrations means that two different types of molecular arrangements of the DMSO molecules are present in the intercalate. The ratio of the two types of molecules is ∼1:3. The Raman spectra differ from that previously published.[22] Multiple bands were found by Johnston et al.[22] at 637, 673, 688, 705, and 720 cm^{-1}. The explanation of some of these bands was not given.

The bands in the Raman spectrum of DMSO at 382 and 333 cm^{-1} are assigned to the in-plane and out-of-plane C−S═O bends (Figure 10). Details of the band component analysis of the Raman and DRIFT spectra of the S═O and C−S bending region of DMSO, DMSO intercalated low-defect kaolinite, and DMSO intercalated high-defect kaolinite are reported in Table 8. The band at 304 cm^{-1} is attributed to the C−S−C symmetric bend.[31−34] The bands assigned to the C−S═O and C−S−C bending modes move to higher frequencies upon intercalation of the kaolinite with DMSO. The C−S−C band is observed at 319 cm^{-1}. The two C−S═O bends are now observed at 355 and 387 cm^{-1}. The bandwidths for the pure DMSO of the 382 and 332 cm^{-1} bands are 12.3 and 15.2 cm^{-1}, respectively. The C−S−C band for DMSO at 304 cm^{-1} has a bandwidth of 17.4 cm^{-1}. Upon intercalation, these three bands have bandwidths of 6.1, 10.5, and 9.3 cm^{-1}. All three bands have decreased bandwidths upon intercalation of the kaolinite. This decrease is significant in that the DMSO is being held in a more rigid crystal-like structure in the intercalate. The intensity ratio of these three bands in the order 382/333/304 cm^{-1} is 1:4:2 for the DMSO and is 4:10:1 for the DMSO in the low-defect intercalate. There is a very large increase in intensity of the in-plane and out-of-plane C−S═O bends relative to the intensity of the C−S−C band. This apparent increase may result from changes in symmetry of the S═O unit in the DMSO intercalation complex. The spectra in this region for the DMSO intercalated high-defect kaolinite are substantially different. The relative intensity of the Raman spectrum of the C−S−C symmetric bending mode is 34.3% compared with the 14.7% for the intercalated low-defect kaolinite. The conclusion is reached that the DMSO molecule is more perturbed for the low-defect kaolinite−DMSO intercalate. For the high-defect kaolinite, the CSC symmetric bend is not as perturbed and so its symmetry is retained and consequently the relative intensity of this band is higher. The C−S═O symmetric bend relative intensity is 46.5% for the DMSO intercalated low-defect kaolinite and 40.2 for the high-defect kaolinite. The significance of the value for the low-defect kaolinite rests with the argument that the C−S═O bend is highly symmetric. Such a molecular arrangement would be possible if the S═O was linearly hydrogen bonded to the hydroxyls of the gibbsite-like surface.

Proposed Model. Figure 11 displays possible models for the interactions between the kaolinite gibbsite-like surface and the DMSO and water. The results of the simultaneous TG−DTG−DTA experiments show that there is one mole of DMSO per mole of inner-surface hydroxyl groups present in the intercalation complex. Therefore, every inner-surface hydroxyl group is individually hydrogen bonded to one DMSO molecule. The hydrogen bonded interactions between the DMSO S═O units and the inner-surface hydroxyl groups are shown as bold dotted lines. This interaction results in the hydroxyl stretching frequencies of 3660 cm^{-1} for the low-defect kaolinite and 3664 cm^{-1} for the high-defect kaolinite. These interactions are envisaged to be orientation dependent and may occur as linear or bent hydrogen bonds. Such orientation dependence was first suggested by Johnston et al.[22] The present model is at variance

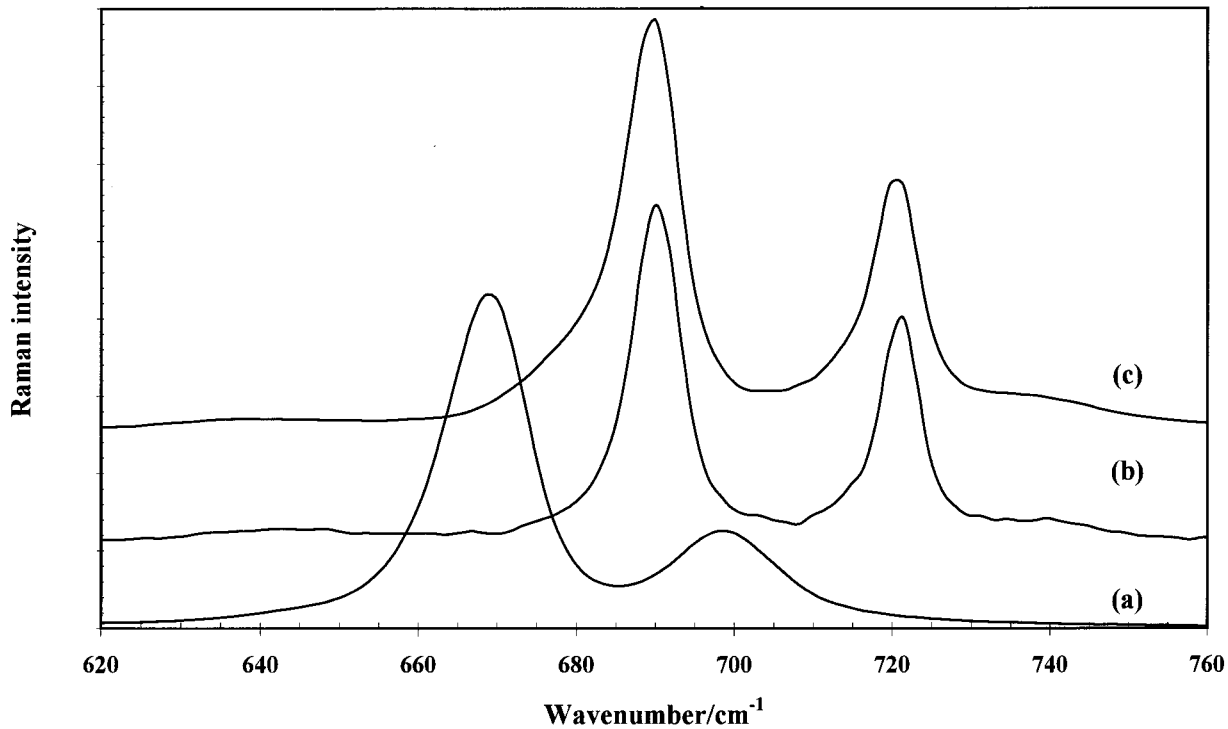

Figure 9. Raman spectra of the C−S stretching region of (a) DMSO, (b) DMSO intercalated low-defect kaolinite, and (c) DMSO intercalated high-defect kaolinite.

TABLE 7: Band Positions, Half Widths, and Band Areas of the Raman Spectrum of the C−S Stretching Region of (a) DMSO, (b) Low-Defect Kaolinite Intercalated with DMSO, (c) High-Defect Kaolinite Intercalated with DMSO

sample	band center cm^{-1}	band widths cm^{-1}	% area
Raman Spectrum of the C−S Stretching Region of DMSO			
ν_{SC-sym}	669	12.6	77
$\nu_{SC-antisym}$	699	15.9	23
Raman Spectrum of the C−S Stretching Region of DMSO in Low-Defect Kaolinite Intercalated with DMSO			
ν_{SC-sym}	690	7.2	60.3
$\nu_{SC-antisym}$	721	5.8	39.7
Raman Spectrum of the C−S Stretching Region of DMSO in High-Defect Kaolinite Intercalated with DMSO			
ν_{SC-sym}	690	7.8	47.8
$\nu_{SC-sym-a}$	680	15.4	15.4
$\nu_{SC-antisym}$	720	6.7	4.2
$\nu_{SC-antisym-a}$	712	14.6	32.6

with the model in which one DMSO molecule is hydrogen bonded to three inner-surface hydroxyl groups.[9]

Importantly in the proposed model, it is suggested that water plays an integral part in the intercalation process—the water molecule acts as the linkage between adjacent DMSO molecules. Hydrogen bonds are formed between the water OH and the lone pairs of the S of the DMSO molecule. Two water hydroxyl groups link two DMSO molecules and form "polymeric" DMSO. This is shown as type 1 DMSO complex in Figure 11. This then results in the band formed at ∼1029 cm^{-1} attributed to polymeric S═O units in DMSO. For the DMSO intercalated low-defect kaolinite, two S═O stretching bands were observed at 1023 and 1010 cm^{-1}. This indicates that two types of polymeric behavior of the inserting DMSO are involved in the intercalate. A second type of interaction occurs when single monomeric DMSO molecules hydrogen bond to the kaolinite inner-surface hydroxyl layer. This is shown as type 2 DMSO complex in Figure 11. Two types of arrangements are recognized: (1) DMSO molecules which are not hydrogen bonded with water (type 3 DMSO complex), and (2) DMSO molecules which are hydrogen bonded to water either through one or both of the water OH groups. For the low-defect DMSO intercalated kaolinite, a band was observed at 1066 cm^{-1}. Such a band was attributed to monomeric DMSO molecules. For the high-defect DMSO intercalated kaolinite, two bands were observed at 1058 and 1040 cm^{-1}. Both of these bands are attributed to monomeric DMSO, and it is possible that the two frequencies are due to the DMSO with and without hydrogen bonded water molecules.

The loss of degeneracy of the C−H stretching vibrations suggests the methyl groups are locked into a rigid structure. Such observations have been determined using NMR spectroscopy.[10−11] While DMSO has two Raman bands at 2911 and 2996 cm^{-1}, upon intercalation of the DMSO into kaolinite, the first band loses degeneracy and splits into two bands at 2917 and 2935 cm^{-1} and the second into four bands at 2998, 3015, 3021, and 3029 cm^{-1}. The blue shift of the C−H stretching vibrations suggests the interactions on the C−H have been reduced. In the model, the DMSO molecules are shown as parallel to the 001 plane. However, some of the C−H may point toward and interact with the siloxane surface.

Conclusions

A new interpretation of the hydroxyl stretching frequencies based on the presence of water in the DMSO intercalate of kaolinite is proposed. Evidence for two types of intercalated water for the low-defect kaolinite and three types of water for the high-defect kaolinite is obtained. Also, evidence for the presence of two types of DMSO molecules in the intercalate is obtained as well. These are monomeric and polymeric molecules. A simple interpretation of only one type of intercalating molecule is rejected. Only one new hydroxyl deformation mode was observed upon intercalation, supporting the concept of one S═O hydrogen bonded inner-surface hydroxyl group. Significantly, the DMSO bands show a decrease in bandwidth upon intercalation; such a decrease is attributed to a crystal-like rigid

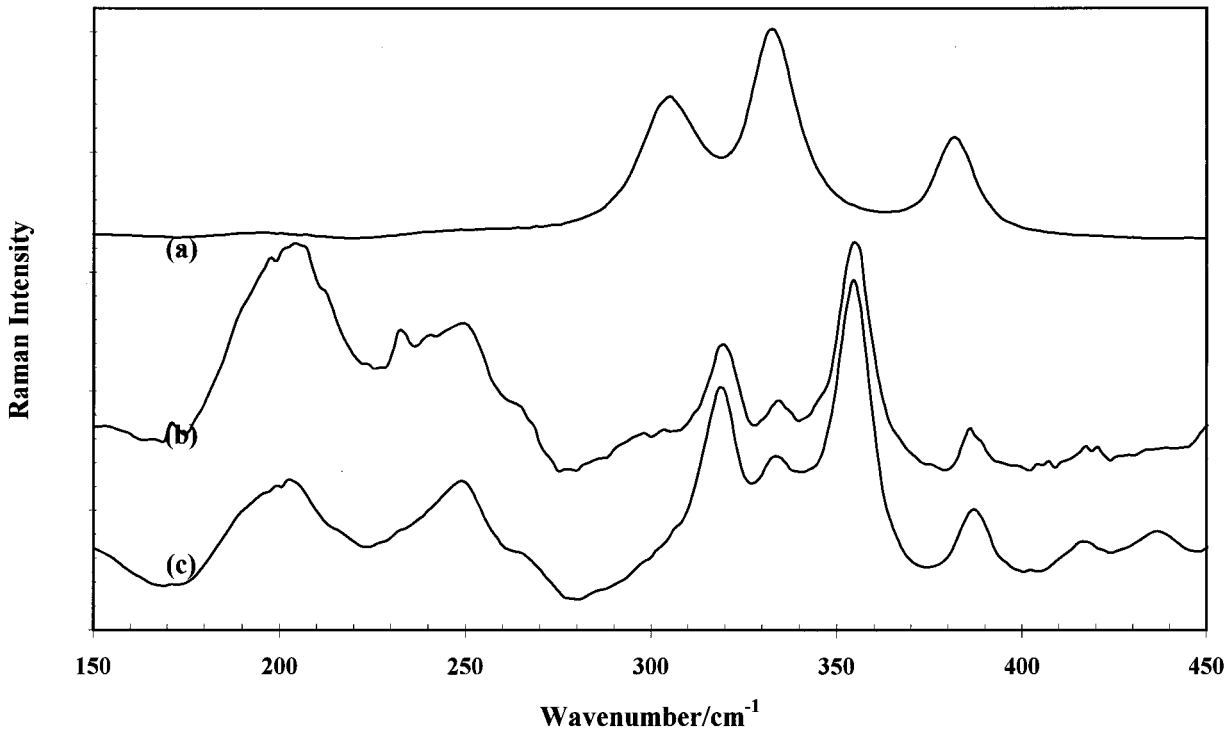

Figure 10. Raman spectra of the C−S−C and S═O bending region of (a) DMSO, (b) DMSO intercalated low-defect kaolinite, and (c) DMSO intercalated high-defect kaolinite.

TABLE 8: Band Positions, Half Widths, and Band Areas of the Raman Spectrum of the C−S═O and C−S−C Bending Region of (a) DMSO, (b) Low-Defect Kaolinite Intercalated with DMSO, (c) High-Defect Kaolinite Intercalated with DMSO

sample	band center (cm^{-1})	band widths (cm^{-1})	% area
C−S═O and C−S−C Bending Region of DMSO			
ν_{CSC}	304	17.4	28.5
$\nu_{S=O\ anti}$	332	15.2	53
$\nu_{S=O\ sym}$	382	12.3	18.4
C−S═O and C−S−C Bending Region of DMSO in Low-Defect Kaolinite Intercalated with DMSO			
ν_{CSC}	319	9.3	14.7
$\nu_{S=O\ sym}$	355	10.5	46.5
$\nu_{S=O\ anti}$	387	6.1	3.8
C−S═O and C−S−C Bending Region of DMSO in High-Defect Kaolinite Intercalated with DMSO			
ν_{CSC}	318	13.7	34.3
$\nu_{S=O\ sym}$	354	12.3	40.2
$\nu_{S=O\ anti}$	387	12.3	11

structure of the DMSO in the intercalate. The bandwidths of the C−H vibrational modes are broader for the DMSO intercalate of the high-defect kaolinite compared with those of the DMSO intercalate of the low-defect kaolinite. It is proposed that the intercalation of the high-defect kaolinite is different from the intercalation of the low-defect kaolinite. The DMSO is not in as rigid a structure for the high-defect kaolinite.

Pronounced changes in the Raman spectra of the inserting molecule are noted upon intercalation of the kaolinite with DMSO. Splitting of all of the symmetric and antisymmetric modes occurs. Such an observation confirms that more than one type of DMSO molecule is present in the intercalate. The S═O symmetric stretching frequencies confirms the presence of three types of DMSO molecules in the intercalate including monomeric, polymeric, and non-bonded DMSO. The concept of different types of DMSO molecules is supported by the complexity of the 950 to 1150 cm^{-1} region where S═O symmetric stretching and the methyl-rocking vibrations occur.

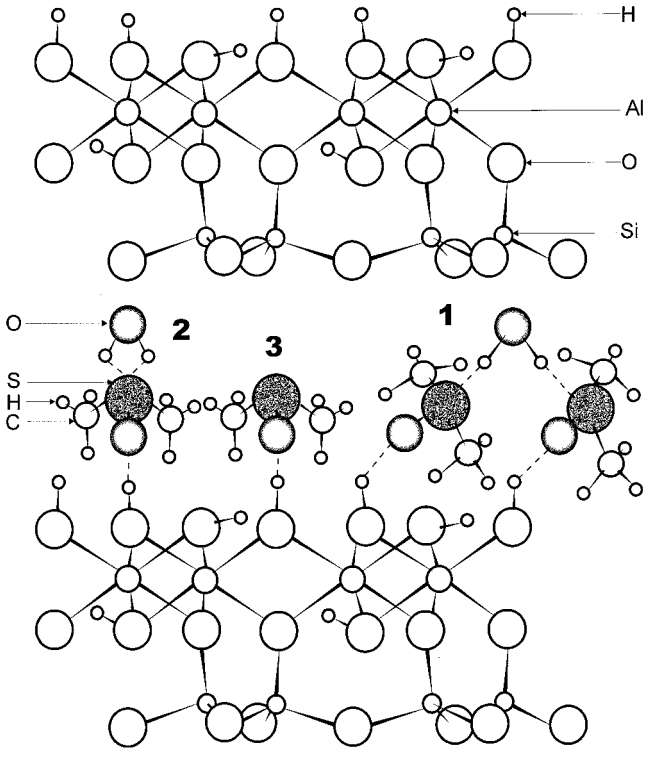

Figure 11. Model of the interactions of DMSO and the kaolinite surface.

The C−H bending region also shows complexity, thus indicating many types of methyl groups in the intercalating DMSO. Whereas for the ordered kaolinite these bands were very sharp, for the disordered kaolinites the bands are broad. Such bandwidths would imply that the intercalation of the disordered kaolinite is different from that of the ordered kaolinite. It is suggested that the ordered kaolinites have a rigid three-dimensional structure whereas the high-defect kaolinites show a less rigid structure.

Acknowledgment. The financial and infra-structure support of the Queensland University of Technology Centre for Instrumental and Developmental Chemistry is gratefully acknowledged. Commercial Minerals (Aust) Pty Ltd is thanked for financial support through Mr. Llew Barnes, Chief Geologist. Financial support from the Hungarian Scientific Research Fund under Grant OTKA T25171 is also acknowledged.

References and Notes

(1) Gonzalez Garcia, S.; Sanchez Camazano, M. *Clay Miner*. **1968**, *7*, 447.
(2) Kirkman, J. H. *N. Z. J. Sci*. **1974**, *17*, 503.
(3) Lim, C. H.; Jackson, M. L.; Higashi, T. *Soil Sci. Soc. Am. J.* **1981**, *45*, 433.
(4) Churchman, G. J. *Clays Clay Miner*. **1990**, *38*, 591.
(5) Heller-Kallai, L.; Huard, E.; Prost, R. *Clay Miner*. **1991**, *26*, 245.
(6) Lapides, I.; Lahav, N.; Michaelian, K. H.; Yariv, S. *J. Therm. Anal*. **1997**, *49*, 1423.
(7) Lahav, N. *Clays Clay Miner*. **1990**, *38*, 219.
(8) Raupach, M.; Barron, P. F.; Thompson, J. G. *Clays Clay Miner*. **1987**, *35*, 208.
(9) Thompson, J. G.; Cuff, C. *Clays Clay Miner*. **1985**, *33*, 490.
(10) Hayashi, S. *Clays Clay Miner*. **1997**, *45*, 724.
(11) Hayashi, S. *J. Phys. Chem*. **1995**, *99*, 7120.
(12) Duer, M. J.; Rocha, J.; Klinowski, J. *J. Am. Chem. Soc*. **1992**, *114*, 6867.
(13) Lipsicas, M.; Raythatha, R.; Giese, R. F., Jr.; Costanzo, P. M. *Clays Clay Miner*. **1986**, *34*, 635.
(14) Thompson, J. G. *Clays Clay Miner*. **1985**, *33*, 173.
(15) Costanzo, P. M.; Giese, R. F., Jr.; Clemency, C. V. *Clays Clay Miner*. **1984**, *32*, 29.
(16) Costanzo, P. M.; Giese, R. F., Jr. *Clays Clay Miner*. **1986**, *34*, 105.
(17) Costanzo, P. M.; Giese, R. F., Jr. *Clays Clay Miner*. **1990**, *38*, 160.
(18) Frost, R. L.; Tran, T. H.; Kristof, J. *Vib. Spectrosc*. **1997**, *13*, 175.
(19) Frost, R. L.; Tran, T. H.; Kristof, J. *Clay Miner*. **1997**, *32*, 587.
(20) Frost, R. L.; Kristof, J. *Clays Clay Miner*. **1997**, *45*, 68.
(21) Olejnik, S.; Aylmore, L. A. G.; Posner, A. M.; Quirk, J. P. *J. Phys. Chem*. **1968**, *72*, 241.
(22) Johnston, C. T.; Sposito, G.; Bocian, D. F.; Birge, R. R. *J. Phys. Chem*. **1984**, *88*, 5959.
(23) Anton, O.; Rouxhet, P. G. *Clays Clay Miner*. **1977**, *25*, 259.
(24) Frost, R. L.; Shurvell, H. F. *Clays Clay Miner*. **1997**, *45*, 68.
(25) Frost, R. L.; Van Der Gaast, S. J. *Clay Miner*. **1997**, *32*, 293−306.
(26) Kristof, J.; Frost, R. L.; Felinger, A.; Mink, J. *J. Mol. Struct*. **1997**, *41*, 119.
(27) Raupach, M. *J. Colloid Interface Sci*. **1988**, *121*, 476.
(28) Yariv, S. *J. Chem. Soc. Faraday 1* **1975**, *71*, 674.
(29) van der Marel, H. W.; Beutelspacher, H. Atlas of infrared spectroscopy of clay minerals and their admixtures. Elsevier: Amsterdam, The Netherlands, 1976.
(30) Rintoul, L.; Shurvell, H. F. *J. Raman Spectrosc*. **1990**, *21*, 501.
(31) Raman, K. V.; Singh, S. *J. Mol. Struct*. **1989**, *194*, 73.
(32) Raman, K. V.; Singh, S. *J. Raman Spectrosc*. **1989**, *20*, 169.
(33) Sastry, M. I.; Singh, S. *J. Raman Spectrosc*. **1984**, *15*, 80.
(34) Singh, S.; Krueger, P. J. *J. Raman Spectrosc*. **1982**, *13*, 178.